Polymer 240 (2022) 124480

Contents lists available at ScienceDirect

Polymer

journal homepage: www.elsevier.com/locate/polymer

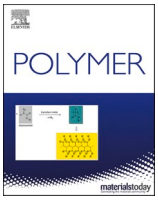

In situ polymerisation of stereospecific propylene nanocomposites blends. Optimising mechanical properties

Karina Núñez [a,*], Paolo Tanasi [a], Maria Asensio [a], Manuel Herrero [a], Luis E. Alonso [b], Julia Guerrero [a], José María Pastor [a,b]

[a] Foundation for Research and Development in Transport and Energy (CIDAUT), Parque Tecnológico de Boecillo, Plaza Vicente Aleixandre Campos N°2, Valladolid, 47051, Spain

[b] Department of Condensed Matter Physics, University of Valladolid, Paseo del Cauce, Valladolid, 47010, Spain

ARTICLE INFO

Keywords:
Polypropylene
Nanocomposites
Metallocenic catalyst
In-situ polymerisation
Mechanical properties

ABSTRACT

Isotactic (iPP) and syndiotactic (sPP) polypropylene composites and their blends containing different amounts of nanosepiolite as cocatalyst support were prepared via in-situ polymerisation using different metallocene catalysts to find out improvements in the mechanical properties in comparison with traditional PP nanocomposites obtained by melt.

The results showed that the amount of nanoclay significantly affects the catalytic activity of the C_s-symmetry catalyst, obtaining nanocomposites with important microstructural changes: increased molecular weight and syndiotactic sections, narrower molecular weight distributions and increased crystallinity. The particular ordering of the crystalline sections of the sPP observed in the WAXS patterns was the main reason for the dramatic changes in the thermal and mechanical properties of the obtained nanocomposites. Although the nanocomposites obtained with catalyst mixtures maintained certain thermal properties of the iPP, these did not translate into improved mechanical properties due to the loss of crystallinity and the preference for the synthesis of syndiotactic configurations.

1. Introduction

Since the 1990s, efforts have been made to explore the benefit of using polymer nanocomposites to have reinforced polymers without a considerable increase in weight [1,2] This has been based on the idea that fillers with large surface area (at least one of their dimensions in nanometer size) have a high effectiveness since they maximize the particle-matrix contact, without the need to use large amounts of reinforcements, as long as there is good chemical compatibility, dispersion and distribution of the nanoparticle in the polymer matrix [3,4]. Special interest has been taken in the use of polyolefin-based matrices, due to their price and versatility, especially in isostatic polypropylene (iPP) which is a material widely used in the automotive industry, construction, packaging, etc.

When iPP-based nanocomposites have been prepared, three major strategies have been followed: the simplest and most studied is based on melt intercalation with the use of compatibilizers [5–7], surface modifications on the nanoclay [8–10] or the application of an electric field to nanocomposites [11,12]. All these efforts have been oriented to improve the chemical compatibility between the matrix and the filler and to avoid the formation of aggregates, since this significantly compromises the mechanical behaviour of the composites [13]. The second strategy is oriented to prepare the nanocomposites in solution, in order to penetrate the layers or separate the aggregates from the nanoparticles more efficiently, introducing the dissolved polymeric chains between them, since they have greater mobility. This is a technique that even with very good results has barriers to commercialization (difficult to scale up, excessive use of solvent, etc.) [14,15]. Another efficient methodology is based on in-situ polymerisation, where the reinforcement is present from the synthesis process itself because it is part of the catalytic system, so that polymeric growth on the nanoparticles guarantees their compatibility and dispersion [13,16–19].

The results obtained in recent years in the in-situ polymerisation technique of iPP nanocomposite show that the modulus is significantly increased without compromising the stereospecificity of the molecule and significantly increases the molecular weights, resulting in materials

* Corresponding author.
E-mail address: karnun@cidaut.es (K. Núñez).

https://doi.org/10.1016/j.polymer.2021.124480
Received 24 August 2021; Received in revised form 23 December 2021; Accepted 23 December 2021
Available online 26 December 2021

with high stiffness. Its use makes it possible to obtain composites with a homogeneous distribution of reinforcement, in a wide range of compositions [20,21]. However, although the surface area of these reinforcements is exploited more efficiently, the toughness of the material and the productivity of the reaction are significantly compromised with this technique, even more so in polyolefins as crystalline as iPP [22].

On the other hand, polypropylene can be found in two types of main configurations: isotactic (iPP) and syndiotactic (sPP). The most commercially exploited is the isotactic one, due to its high crystallization capacity, which gives it mechanical properties far superior to any other type of polyolefin, making it the most widely consumed at industrial level. The recently obtained sPP with high tacticity and high molecular weight using metallocene catalysts [23] is receiving great attention due to its particular properties for use as gels [24], as a semicrystalline polymer with memory effect [25] or thermoplastic elastomer [23,26]. All this is due to a very complex polymorphic behaviour that is still being studied [27–29]. From an industrial point of view in applications where high mechanical performance is required, its performance is not as good as that of isotactic polypropylene, but this makes the preparation of sPP blends [30] and nanocomposites very attractive to improve its competitiveness and improve the toughness problems presented by iPP nanocomposites.

Most of the works reported in the literature with respect to sPP nanocomposites refer to melt processing with the use of compatibilizers, because like iPP, sPP is a non-polar structure. In these works, particles such as nanoalumina have been used, showing a significant increase in the crystallization rate of sPP in the presence of the nanoparticle, but no significant change in the crystal structure is observed [31]. In the case of the use of nanosilica or carbon nanotubes (CNTs), significant changes in the thermal behaviour of sPP are observed, mainly related to a strong nucleating effect, much higher in CNTs than in nanosilica. In addition, these nanoparticles caused important changes in the rheology, thermal and mechanical behaviour of the sPP [32]. Other authors have used lamellar nanoclays in sPP of different characteristics and molecular weight and showed that there was a good distribution of the nanocarbon, dependent on the initial characteristics of the sPP and an increase of the mechanical properties [33–36]. Additionally, lamellar clays such as bentonite or montmorillonite affect the dimensions and parameters of the chains and consequently the whole chain dynamics (molecular weight of entanglements such as packing length) in sPP nanocomposites obtained by melt technique [37,38].

There is practically no literature concerning in-situ polymerisation of sPP nanocomposites, although Polshchikov and co-workers [39] showed that in-situ polymerisation of sPP in the presence of carbon nanotubes did not lead to a significant decrease in the activity and stereospecificity of a syndiotactic catalyst. The mechanical behaviour of other types of sPP nanocomposites remains to be investigated.

In this work we studied for the first time the possibility of achieving a compromise of mechanical properties in PP matrix nanocomposites of different stereoregularities (iPP, sPP and mixtures thereof) by supporting metallocene co-catalyst (MAO) in fibrillar nanoclay, which were used at the same time as reinforcement.

2. Experimental

2.1. Materials

The polymerisation gas used was propene (supplied by Air Liquide). This gas is polymerisation grade, with less than 0.06 ppm of oxygen and 0.4 ppm of nitrogen. The following compounds were part of the catalyst system employed: dimethylsilylbisbenzyl zirconium (IV)-dichloride ($Me_2Si(Ind)_2ZrCl_2$, Aldrich) and diphenylmethylidene (cyclopentadienyl) (fluorenyl) zirconium dichloride $Ph_2C(Flu)(Cp)ZrCl_2$, Aldrich); which were used as catalysts. Methylaluminoxane (MAO, 17 wt% solution in toluene, AzkoNobel) or Tri*iso*butylaluminium (TIBA, 25 wt% solution in toluene, Sigma-Aldrich) were used as co-catalyst or cleaning agent, respectively. All were used without any treatment. The solvents (Toluene, Fisher Scientific).

The clay used for the preparation of metallocene PP nanocomposites was a commercial sepiolite (SEP) supplied by TOLSA (unit fibre size 0.2–3 μm, 10–30 nm width, and 5–10 nm in thickness), the physical-chemical properties of the sepiolite fibre bundles are shown in Table 1. These fillers were dried under vacuum at 80 °C for 24 h before treatment.

All materials sensitive to air, water and impurities were handled in an inert atmosphere under a flow of Nitrogen (99% purity, Air Liquide) within a glove box or inside the polymerisation reactor, respectively.

The Physical-Chemical Properties of Sepiolite were privately provided by TOLSA.

2.2. Clay treatment

The desired amount of dry clay was mixed with co-catalyst, in ratio 2 g clay/ml of MAO solution, in 100 ml of dry toluene and afterward the mixture was stirred for 90 min at room temperature, following the procedure explained in our previous works for optimizing the process of immobilization of the MAO in sepiolite [17,22,40]. The resulting solid was washed three times with 30 ml of fresh toluene and dried inside glove box until it was used.

As it was reported in a previous work [40,41] the sepiolite reacts with MAO to form a covalent (Al–O) binding between the Aluminium from MAO and the hydroxyl group (-OH) from sepiolite surface, which acts as a Brønsted acid. In this study, the vibration corresponding to the Si–O–Al bond (1015 cm^{-1}) present in the treated sepiolites was identified by FTIR as proof of the effective covalent binding between the MAO and the Silanol groups on the surface of the sepiolite.

2.3. Polymerisation

Polymerisation of different neat polypropylenes (iPP, sPP and iPP + sPP) was carried out following a rigorous cleaning process of the reactor. The polymerisation temperature was set at 20 °C, once achieved, 0.05 M solution of TIBA in toluene was transferred to the reactor and kept under propene atmosphere stirring for 5 min at 600 rpm. In a second step, the reactor was fed with 3.0×10^{-6} mol of a stereo-specific catalyst in 100 ml of toluene and the amount of MAO solution suitable to have an Al/Zr ratio of 1:1200. The reaction started with the propene injection at 5 bars and held for 1 h.

Equal amounts of each catalyst were used when both catalysts were mixed (iPP + sPP). The amount of total Zr moles was maintained (3.0×10^{-6} mol) as in all other reactions where a single catalyst was used.

The catalytic activity was stopped by hydrolysing the MAO with the addition of 100 ml of a mixture of ethanol and 10 %v of hydrochloric acid. The polymer was precipitated in 800 ml of water and kept under stirring for 12 h. It was finally filtered and dried at 80 °C under vacuum for another 12 h approximately.

All materials (iPP, sPP and iPP + sPP) were polymerized with different initial amounts of treated nanoclay (0.5 y 1 g) to obtain their corresponding nanocomposites: N0.5iPP, N1sPP, N0.5sPP, N1sPP, N0.5 (iPP + sPP) and N1 (iPP + sPP). These nanoparticles were added in the second stage of the described polymerisation protocol together with the

Table 1
Physic-chemical properties of sepiolite for fibre bundles.

	Composition	BET Specific surface area (m^2/g)	Average particle size – laser granulometry (μm)
Physical chemical properties	Magnesiun silicate $Si_{12}O_{30}Mg_8(OH)_4(H2O)_{4\cdot 8}H_2O$ Impurities: Al_2O_3<5%, Fe_2O_3<2%	319	12.69 50% < 8.71 μm 90% < 29.72 μm

corresponding catalyst.

2.4. Sample preparation

The obtained nanocomposites were homogenised with two thermal stabilizers for polyolefins (Irganox 1010 and Irgafos 168 supplied by Ciba, Spain) during extrusion process at 210 °C/80 rpm. At a later stage were moulded in a Schwabenthan hot plate press, heating at 200 °C, for 5 min without pressure and the second step was applied 10 MPa with an additional 10 min. Finally, the plates were stamped with the specific dimensions for each characterization test.

2.5. Characterization

In a polymerisation process, the most important characteristic parameter is productivity. The productivity was measured as (kilograms of polyolefin)/(Zr moles x pressure x time).

The melt and crystallization temperatures (T_m, T_c), as well as the heat of melt (ΔH_m) and degree of crystallinity of samples (X_c), were measured by a Mettler Toledo DSC 821e thermal analysis system model (DSC) in the temperature range from 25 to 250 °C at a heating rate of 20 °C min^{-1} under nitrogen flow. The samples were first heated to 250 °C for 2 min to eliminate their thermal history and subsequently cooled to 25 °C. The second endotherm was recorded by heating 20 °C min^{-1}. The reported data are from the second melting endotherm. Calculation of the degree of crystallinity of iPP ($X_{c,\ iPP}$) and sPP ($X_{c,sPP}$) has been done as Equations (1) and (2), where ΔH_m is the melting enthalpy (area of the melting endotherm. In both pure materials and mixtures only one endotherm appears on the DSC curves). $\Delta H^{\circ}_{m,iPP}$ and $\Delta H^{\circ}_{m,sPP}$ are the melting enthalpies of iPP and sPP exhibiting 100% crystallinity and equaling 209 and 196 J/g respectively [42]. 'wt% iPP' and 'wt% sPP' are the mass composition of the mixture obtained by ^{13}C NMR test. The degree of crystallinity of the blends has been calculated as follows (Equation (3)):

$$X_{c,iPP} = \frac{\Delta H_m}{\Delta H^{\circ}_{m,iPP}.wt\%_{iPP}} \quad (1)$$

$$X_{c,sPP} = \frac{\Delta H_m}{\Delta H^{\circ}_{m,sPP}.wt\%_{sPP}} \quad (2)$$

$$X_{c,blends} = X_{c,iPP} + X_{c,sPP} \quad (3)$$

Thermogravimetric Analysis (TGA) was used to determine the clay content in the obtained nanocomposites. Thermograms were obtained in a nitrogen atmosphere with a heating rate of 20 °C min^{-1} using a Mettler Toledo TGA851e. The weight percent of clay measurements were taken after a temperature sweep from 50 °C to 950 °C under inert atmosphere and at a rate of 20 °C min^{-1}.

To analyse the formation of nanoparticle aggregates, transmission electron microphotographs (TEM) were taken from 100 nm microtomed sections of the composites cut with a Reichert–Jung Ultracut E microtome using a JEOL JEM 2000FX Electron Microscope with an accelerating voltage of 200 kV.

^{13}C NMR assays were used to determine the tacticity of the synthesized PP, through the identification of the couplings and molecular vibrations of the samples. ^{13}C NMR assays were performed on a 500 MHz NMR Spectrometer (BRUKER AVANCE III 500, 11.74 T. Different concentrations were used depending on the different solubility of the samples. In case of isotactic polypropylene, with or without nanoclay, the concentration used was 100 mg/mL the presence of syndiotactic polypropylene, in the mixtures, meant reducing the concentration by half (50 mg/mL). Finally, in the samples with only syndiotactic polypropylene, the concentration was reduced to 35 mg/mL. The solvent used was 1,2,4-trichlorobenzene at 100 °C. The PerkinElmer Spectrum 100FTIR spectrometer was used to analyse the characteristic bands of iPP (1170 and 1000 cm^{-1}) and sPP (870 cm^{-1}) in the mixtures obtained.

The WAXS measurements were carried out with a Siemens D500 apparatus. For the measurements a CuKα radiation of a wavelength λ = 0.154 nm was used.

Molecular weight distributions were determined with a Waters ALLIANCE GPCV 2000 gel permeation chromatographer (GPC). 1,2,4-trichlorobenzene was used as a solvent, at a flow rate of 1 cm^3 min^{-1}. The nanocomposites were dissolved and filtered through a 0.45 μm PTFE filter to remove the solid particles. The analyses were performed at 145 °C.

The mechanical properties of the resulting nanocomposites were measured as follows: Young's modulus at a speed of 1 mm min^{-1} and tensile strength at a speed of 50 mm min^{-1} were measured according to ISO 527–1. Method A, with an Instron Model 5500R60025. Because of the elastomeric behaviour of pure sPP, compared to the rest of the materials studied, the fixed grips were replaced by pneumatic grips to regulate the pressure and avoid displacement and breakage of the specimen in the gripping zone. The type of specimen used was 1BA in all samples. In order to report specific properties, density was measured using an analytical balance Mettler Toledo, model AX205DR, under the standard ISO 1183–1.

3. Result and discussion

This research aims to improve the ductility of iPP nanocomposites, through the synthesis of polypropylene in its syndiotactic configuration or in a random mix of iso and syndiotactic blends, using a mixture of two stereo-specific metallocene catalysts. The idea is based on preserving the maximum rigidity of iPP nanocomposites but improving deformation capacity (i.e. toughness) with the addition of syndiotactic sections, which reduces crystallinity and make a certain part of the structure behave like a type of thermoplastic elastomer, with good impact absorption. On the other hand, sPP homopolymer is a suitable material to be reinforced with nanofillers by the in-situ method, since being a more ductile and less crystalline material than iPP, it has a lower Young's Modulus. Its polymerisation in the presence of the nanofiller could offset its lack of rigidity to use it in different applications that are in demand today. The in-situ polymerisation method studied here is based on the support of the cocatalyst (MAO) in a fibrillar clay (sepiolite) with a large surface and rich in hydroxyl groups (-OH) to form a strong bind between them (Si–OH; Silanol groups) and with this create polymerisation points of polymeric chains adhered to the nanofiller [40] (see Fig. 1). To verify the advantages of the in-situ polymerisation method, a study of the influence of the nanoparticles on the microstructural properties of the various nanocomposites obtained has been carried out.

3.1. Microstructure of the obtained nanocomposites

^{13}C NMR spectroscopy in solution has been the technique used to investigate the microstructure of the nanocomposites obtained. The ^{13}C NMR microstructure of a polypropylene sample is a fundamental source of information on its properties, and also a 'fingerprint' of the catalytic species used to produce it [27].

The tacticity of the polypropylenes studied was calculated by analysing the signals corresponding to the methyl region. The analysis has been carried out considering five consecutive monomer units, i.e. at the pentad level, which allows the determination of ten different sequences depending on the methyl orientation (Fig. 2). Table 2 shows the results of the tacticity analysis carried out. In the supporting information the obtained spectrums are shown.

The results show the high stereospecificity of the catalysts used and the formation in-situ of a mixture of two clearly separated stereoregular sections when the catalysts are mixed. This is explained by the fact that the main sequences formed were of the rrrr (C) or mmmm (J) type (see Table 3). There is about 10% of non-stereoscopic configuration in all the samples analysed, corresponding to the atactic fractions. These sections

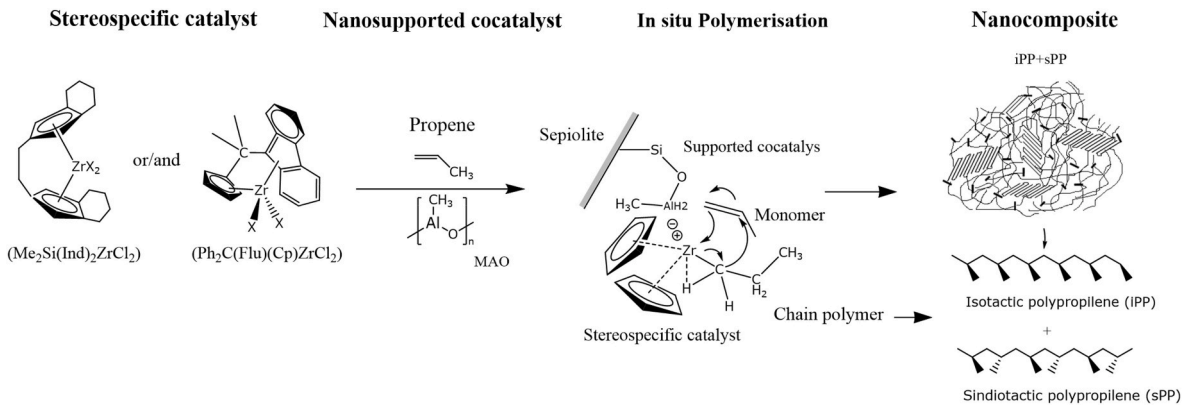

Fig. 1. Scheme for obtaining iPP, sPP, and iPP + sPP nanocomposites.

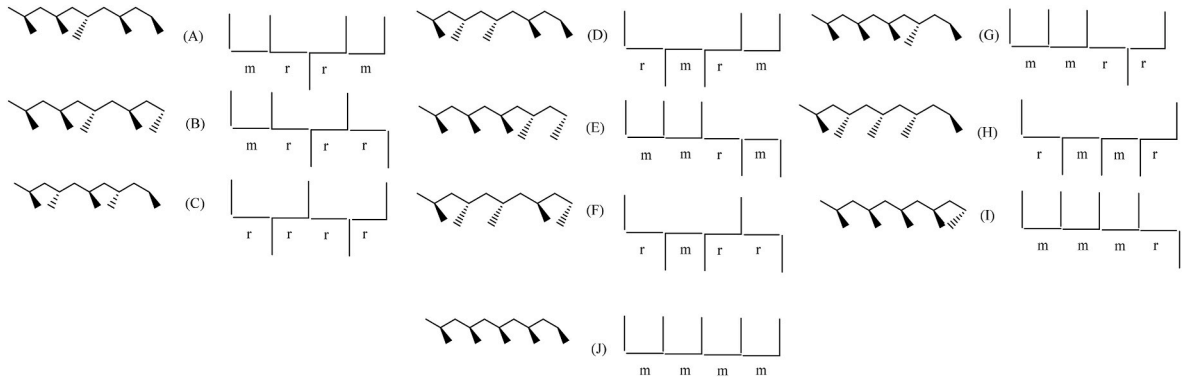

Fig. 2. Saw-horse and Fischer projections of regioirregular studied sequences.

Table 2
Tacticity analysis of iPP, sPP, iPP + sPP and their nanocomposites.

Sequence	iPP		N1iPP		sPP		N1sPP		iPP + sPP			N1(iPP + sPP)		
	δ(ppm)	%	δ(ppm)	%	δ(ppm)	%	δ(ppm)	%	δ(ppm)	δ(ppm)	%	δ(ppm)	δ(ppm)	%
(A) PPPPP(mrrm)	19.557	0.9	19.553	0.9	19.771	4.5	19.490	1.1	–	19.507	1.0	–	19.505	0.6
(B) PPPPP(mrrr)	–	–	–	–	19.825	3.7	19.533	1.0	19.825	19.770	1.5	19.820	19.767	3.9
(C) PPPPP(rrrr)	–	–	–	–	19.962	**82.0**	19.678	**95.9**	–	19.959	**39.7**	–	19.955	**61.5**
(D) PPPPP(mrmr)	–	–	–	–	–	–	–	–	–	–	–	–	–	–
(E) PPPPP(mmrm)	–	–	–	–	–	–	–	–	–	20.477	1.0	–	20.473	0.8
(F) PPPPP(rmrr)	–	–	–	–	20.478	2.4	20.195	0.7	–	–	–	–	–	–
(G) PPPPP(mmrr)	20.732	3.8	20.734	1.7	20.686	3.7	20.401	0.3	20.683	20.712	3.0	20.678	20.706	3.0
(H) PPPPP(rmmr)	–	–	–	–	20.971	2.3	20.690	0.6	–	20.971	1.0	–	20.967	1.1
(I) PPPPP(mmmr)	21.301	3.1	21.544	1.1	–	–	–	–	–	21.249	2.5	–	21.246	1.4
(J) PPPPP(mmmm)	21.572	**90.7**	21.544	**95.4**	21.530	0.8	21.242	0.3	–	21.522	**50.3**	–	21.518	**27.7**

remained practically invariant in the nanocomposites.

The increase in the stereospecificity of the synthesized nanocomposites, compared to pure materials, may be due to the stability that the sepiolite confers on the catalyst system, by protecting the active centres, that are on the surface of the support. This is possibly due to the fact that under these reaction conditions, a slow and coordinated synthesis is promoted, because an ideal homogeneous catalysis with a single active site is promoted, as we have reported in previous work [22].

Although it can be thought that the presence of clay in the nanocomposites could represent a steric impediment for the rotation and the controlled insertion of the monomer in the growing chain, at low nanoclay concentrations, the coordinated activity of the stereospecific C_2 and C_s-symmetry catalysts is not affected. In contrast, the stereoregularity of iPP and sPP nanocomposites increases to almost 96%. This is due to the stability provided by immobilization of the catalyst on a solid particle [43,44]. Remarkably, the stereospecificity of the sPP nanocomposite increased by 14% compared to neat sPP. A result that is not possible to achieve in iPP nanocomposites, where the isotacticity of the homopolymer was already very high (90.6%), and yet it has increased by 5%. The nanoclay enhances the control mechanism of the enantiomorphic site of the C_s-symmetry catalyst, which promotes repulsive interactions that force the monomer to approach the active site of the catalyst with the enantiotropic side, increasing its syndiotacticity, as described by Caporaso and Cavallo [51,52] in their molecular mechanics studies.

When studying the materials obtained with the mixture of catalysts, it is observed, as expected, that in the one without clay (iPP + sPP), 50% of syndiotactic sections and 40% of syndiotactic sections are obtained, with about 10% of non-specific sequences. In work by Kaminsky and López-Moya [53,54] it has been reported that a high stereotactic control of the C_2-symmetry catalyst when it is together with the C_s-symmetry catalyst. The latter could be acting as an isospecific catalyst due to steric

Table 3
Composition and thermal properties of iPP, sPP and iPP + sPP nanocomposites obtained with different initial amounts of sepiolite.

Sample[a]	T_m (°C)[b]	T_c (°C)[b]	ΔH_m (J/g)[b]	X_c (%)[b]	wt. % Final nanoclay[d]	*Productivity kg PP/mol Zr . h . bar.*
iPP	147.9	102.4	165.1	78.9	–	$5.62 \times 10^3 \pm 2 \times 10^2$
N0.5iPP	148.8	104.6	171.1	81.8	1.1 ± 0.2	$5.32 \times 10^3 \pm 2 \times 10^2$
N1iPP	149.3	108.6	173.4	82.9	1.6 ± 0.2	$4.93 \times 10^3 \pm 2 \times 10^2$
sPP	134.3	79.7	52.92	27.0	–	$6.25 \times 10^3 \pm 1 \times 10^2$
N0.5sPP	140.6	86.1	76.44	39.0	1.3 ± 0.1	$4.61 \times 10^3 \pm 1 \times 10^2$
N1sPP	146.6	89.5	103.8	52.9	3.2 ± 0.2	$3.23 \times 10^3 \pm 1 \times 10^2$
iPP + sPP	147.0	80.5/ 98.1	91.0 (50% iPP + 40% sPP)[c]	39.9	–	$5.72 \times 10^3 \pm 2 \times 10^2$
N0.5 (iPP + sPP)	147.8	83.1/ 99.3	93.5 (40% iPP + 50% sPP)[c]	41.1	1.4 ± 0.2	$5.26 \times 10^3 \pm 1 \times 10^2$
N1(iPP + sPP)	149.1	90.2/ 102.0	97.1 (30% iPP + 60% sPP)[c]	43.2	2.1 ± 0.1	$4.80 \times 10^3 \pm 1 \times 10^2$

[a] Nomenclature: For N0.5iPP; N (Nanocomposite), 0.5 (Grams of clay added in the reactor), iPP (Corresponds to the stereospecific matrix).
[b] The DSC test have been performance on pellets after a homogenization process in a twin-screw extruder. The reported data are from the second melting endotherm.
[c] Obtained by ^{13}C RMN test.
[d] Obtained by TGA test.

hindrance at the coordination site of the metallocene due to the presence of the other catalyst. Therefore, an intermolecular interaction could be affecting the stereochemistry of the active centre of the C_S-symmetry catalyst and therefore in the blends there is a lower percentage of rrrr sequences.

However, this behaviour is the opposite in the presence of the nanofiller, where the N1(iPP + sPP) nanocomposite prioritises the syndiotactic sections (60%); i.e., as observed in the sPP nanocomposite, the nanoclay encourages the coordination mechanism of the C_s-symmetry catalyst, overcoming the negative influence that the presence of the C_2-symmetry catalyst has shown to have on its activity. This confirms that the in-situ polymerisation mechanism with sepiolite, as a nanofiller, favours the synthesis of syndiotactic sections.

For the FTIR analysis of the fractions, we used the 1170 and 1000 cm^{-1} bands, characteristic of iPP, and the 870 cm^{-1} band, characteristic of sPP [45]. The iPP + sPP spectra show the characteristic bands of both configurations. Invariantly, the same signals appear in their nanocomposite (N1(iPP + sPP)). The unchanged signals demonstrate the separate formation of both sections, which confirms that a mixture, not a stereo-block copolymer, was formed.

3.2. Thermal transitions of the obtained nanocomposite and polymerisation productivity

The results of the characterization of the different nanocomposites (see Table 3) have shown that regardless of the nanocomposite matrix's stereoregularity obtained, a raise in the amount of nanofiller, in the reaction medium, increases both degree of crystallinity (see Fig. 3a) and melting temperatures (see Fig. 3b). In counterpart, increasing the amount of nanoclay in the medium decreases the reaction productivity producing fewer polymeric chains, and thereby increasing the final amount of nanofiller (see Fig. 3c).

In particular, from the thermal tests it can be observed that, compared to iPP, sPP is a material that due to its configuration has a lower degree of crystallinity, as expected, and thereby, a lower melting point is found of more than 10 °C below than that of pure isotactic PP. Regarding the nanocomposites, it is remarkable the notorious nucleating effect that sepiolite has on the structures that are formed, particularly in the syndiotactic configuration. The nanocomposite N1sPP with a 3.2 wt % clay effective load, increases its melting and crystallization temperature by more than 10 °C and its degree of crystallinity by close to 50%, in comparison with its homologous (sPP) without nanofiller. This result is not obtained for iPP and its corresponding nanocomposite (N1iPP), where the increases in these thermal transitions are less marked (see Fig. 3a and b).

These results may be correlated to the final amount of clay in the nanocomposite obtained. Under the same reaction conditions (1 g of initial sepiolite), the N1sPP has a final amount of clay of 3.2 wt%, twice the amount of the N1iPP (1.6 wt%). In addition, this means that the coordination mechanism of the syndiotactic catalyst is more affected by the presence of nanoclay, as shown by the productivity data of the reaction (see Fig. 3c). Although there is very limited literature on this subject, authors such as Kovalchuk et al. [46] have shown that this catalyst maintains its activity invariant during in-situ polymerisation, with an increase in the amount of multi-wall carbon nanotube, in the same proportions as those studied in this work (<4 wt%). With these results, it could be affirmed that the nature and shape of the particles used in-situ polymerisation are determinant in the activity of this C_s-symmetry catalyst.

The hydroxyl groups on the surface of the sepiolite can deactivate the catalyst more easily, therefore less polymer is synthesized and there is more effective loading in the final composite. This final amount of clay may be responsible for the marked nucleating effect in syndiotactic nanocomposites (NsPP), since a higher amount of final clay in the nanocomposite favours important nucleation points, as explained by several authors who have worked by melt techniques [32,35,36].

However, it is important to note that despite the polymerisation reactions with the syndiotactic catalyst, lose productivity in a faster way, with the increase of the nanoclay (see Fig. 3c), it is also true that the pure sPP has the higher productivity than the rest of the configurations. Additionally, in the early stages of the sPP's nanocomposites polymerisation, this configuration is the one that offers the greater polymerisation starting points, since when the monomer consumption flows are measured, the sPP reaction begins with greater speed, i.e., greater gas consumption (see Fig. 3e). Although in the presence of clay, this productivity or consumption of the monomer, falls more abruptly, compared to the other configurations.

The increase in productivity of pure syndiotactic configuration polymerisations has already been reported by other authors [47,48] who show that this is associated with the geometry of the catalyst, with a greater the distance, d, between the center of the cyclopentadienyl rings there is a greater reactivity of the metal center of the catalyst, because the ligament that forms the intermolecular bridge is a diphenylmethyl and this is more voluminous, in syndiotactic catalysts. Despite the fact that this type of catalyst is more active, the results of this work show that, on the other hand, it is the most prone to being deactivated in the presence of the nanosepiolite heteroatoms, which did not react with the cocatalyst, when the in-situ method is applied.

In conclusion, when the results of the thermal characterization of NiPP and NsPP are compared, it can be established that there is an important effect of the initial nanoclay load used in the reaction, and the final amount of nanoclay in the nanocomposite over the crystallization of these materials. In turn, the amount of final reinforcement is conditioned by the stereospecific activity of the catalyst used, having an especially notable effect on nanocomposite sPPs. This means that with

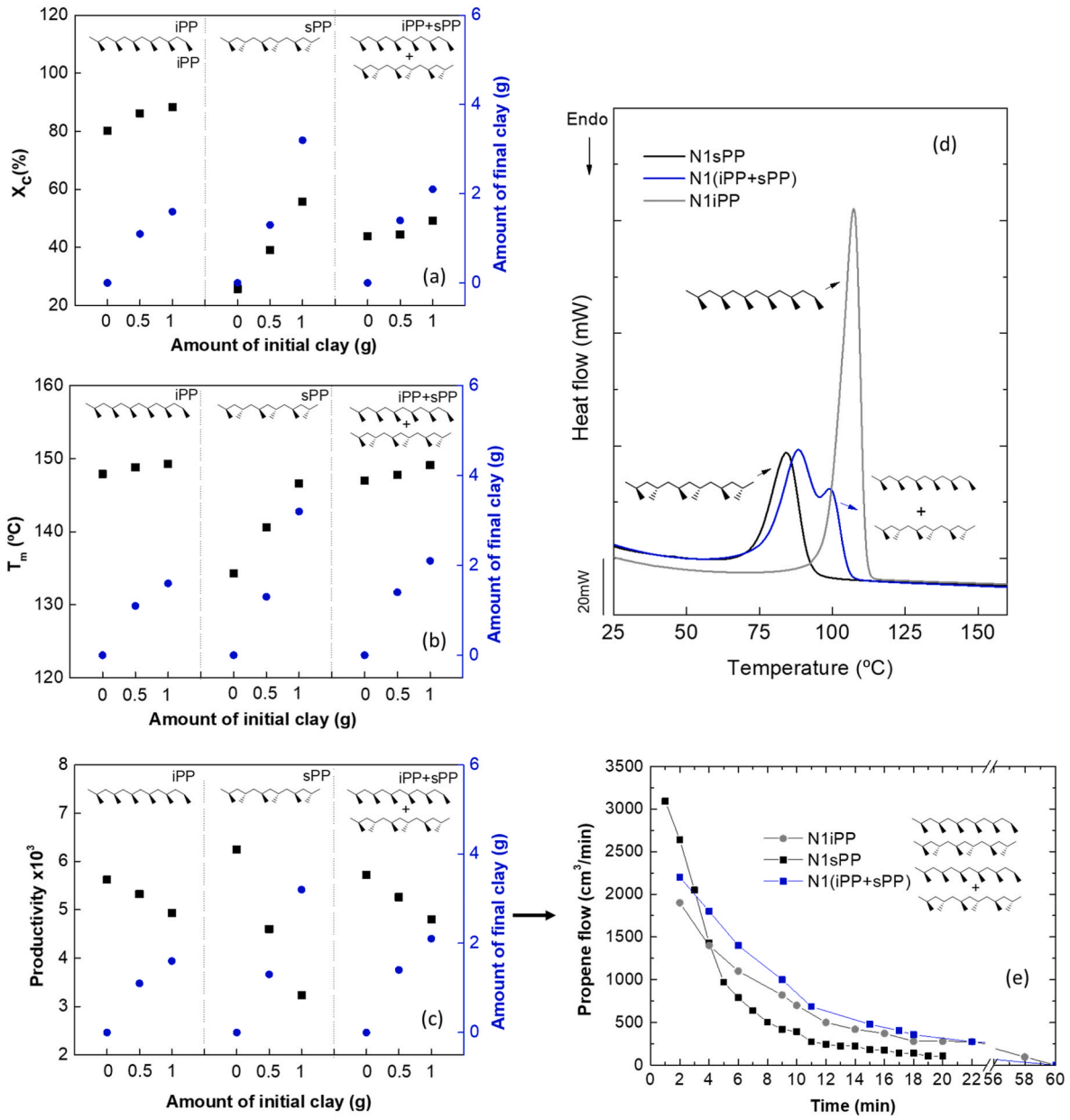

Fig. 3. Influence of the amount of initial clay, in different matrix stereoregularities, with (a) crystallinity percentage, (b) melting temperature and (c) catalyst productivity. (d) crystallization exotherms and (e) propene consumption rate for nanocomposites obtained with 1 g initial clay in different stereoregular matrices.

final amounts of loading of 3.2 wt%, N1sPP can reach similar melting temperatures to those of iPP and its nanocomposites (see Fig. 3b), which is very interesting to improve the rheological and mechanical behaviour of pure sPP.

On the other hand, when the nanocomposites obtained from the mixture of catalysts N(iPP + sPP) are studied, a very similar behaviour is observed with NiPP. As the amount of clay added to the reaction increases there is a drop in productivity with the same slope, which translates into percentages of final nanoclay load, in the nanocomposites, practically the same (see Fig. 3c), although an increase in productivity in the catalyst mixture would have been expected, due to the contribution of each active site. In this regard, the literature reports that, to produce homopolymers with hybrid catalysts, the activity of each active center is random and the productivity of the reaction depends on the interaction between both metallocenes anchored in the support, which in most cases is silica [47,49,50].

In this case the mixture of catalysts is not supported, only the cocatalyst is supported in the nanofiller and the activity seems to rely on the survival of the active centres with the amount of impurities in the polymerisation medium [51]. In this case the impurities are mainly associated with the free –OH groups on the surface of the nanofiller and these increase with the increase of the nanoclay in the medium.

As already mentioned, the syndiotactic catalyst has shown greater sensitivity to the presence of these impurities, so that in the blends and its nanocomposites obtained with the mixture of catalysts N(iPP + sPP), the reaction activity seems to be led by the isotactic catalyst or by the possible interactions that occur between both catalysts, as has been proposed by Marquez et al. [49] (see Fig. 3c).

Additionally, the average melting temperatures between NiPP and N (iPP + sPP) is also very similar (see Fig. 3b). However, when their degree of crystallinity are compared (see Fig. 3a), the nanocomposites N(iPP + sPP) have practically half the crystals as their NiPP homologous. The results obtained show that crystals of the same lamellar size are formed, but in less quantity. This result may be the consequence of the

imposition of a series of negative effects on crystallization: defects in the polymeric sequences (see pentad study by ^{13}C NMR test shown in Table 2) in each PP type obtained in the mixtures (iPP and sPP) that do not allow them to crystallize or that the nanofiller and its possible aggregates act as a defect in the crystalline system. These negative effects seem to domain over the positive effects: the nanofiller can act as a nucleation point and/or fractions of iPP can act as an "inducing crystal" on the sPP phase [47]. This allows us to conclude that it is not possible to achieve synergistic effects in thermal properties, since these do not exceed NiPP values when nanocomposites are synthesized with hybrid catalysts by the in-situ method.

Finally, regarding the thermal properties, when the crystallization exotherm curves are studied for the different configurations of nanocomposites obtained (see Fig. 3d), two crystalline populations are clearly observed in the N1(iPP + sPP), being more predominant the section that is formed at the same crystallization temperatures of the sPP. Furthermore, when comparing the nanocomposites of the blends N (iPP + sPP) with different amount of clay, the nucleating effect of the nanofiller on both configurations can be confirmed, as both fractions increase their T_c as the amount of nanoclay increases (see Table 3). However, a shift to lower temperature is seen for the crystallization of the isotactic fraction in N1(iPP + sPP) when it is compared to N1iPP (see Fig. 3d). The opposite case occurs when comparing the syndiotactic fraction of the mixture to its pure analogue, a rise in Tc is observed (see Fig. 3d). This shows that in either case the crystallization of the syndiotactic fraction is favoured in the in-situ polymerisation studied.

On the other hand, despite the fact that in the exotherms of the nanocomposites, obtained with a mixture of catalysts, two peaks are clearly shown (see Fig. 3d). In the first heating scan, the fusion endotherms of the same nanocomposites show a single peak that narrows as the amount of clay increases (see Fig. 4b) and this phenomenon is also repeated in the NsPP and NiPP (see Fig. 4a and c, respectively). This phenomenon has already been reported in polyolefin nanocomposites by in-situ technique, associating it to the hierarchy of the metallocene catalyst with a single active site [17,22] as the in-situ mechanism significantly narrows the molecular weight distribution and increases the stereoregularity of the matrix.

In the case of the catalyst mixture, we observed that the nanoclay in the polymerisation medium significantly narrows the crystal size distribution, making it impossible to differentiate during merging the two stereospecific sections that are formed (see Fig. 4b).

The significant influence of in-situ polymerisation with fibrillar nanoclay on the sPP matrix can be explained by the WAXS patterns shown in Fig. 5. The pure sPP sample presents typical behaviour with a disordered crystallization with the chains in helical conformation characterised by reflection (020) at $2\Theta = 15.9°$, and (220) at $2\Theta = 20.7°$ [25,34]. Other authors such as Stricker et al. [51] identify this pattern with the unit cell type III, suggesting substantial packing disorder along the b-axis, which is typical of packing mode II [52].

The reflection at $2\Theta = 17.5°$ is absent in the pure sPP sample, but appears with a strong reflection in the nanocomposite, attenuating the rest of the signals. This reflection is typical for the C-centred unit cell type I [52]. The results show that there is a substantial change in the crystallization pattern: a preferential ordering of the crystalline sections is produced.

The opposite effect is reported in the case of sPP nanocomposites obtained in melt where the increase of nanoparticles increases the disorder in the crystalline system [34,36,52]. Our experimentation allows us to conclude that, in the case of matrix sPP, in-situ polymerisation with fibrillar clays narrows the crystalline distribution in size and shape (higher order) and this is also reflected in the significant increases in T_m.

3.3. Molecular weights of the nanocomposites

Fig. 6 shows the results of the GPC tests to monitor the evolution of molecular weight, molecular weight distribution and polydispersity index of the nanocomposite's matrix. The results show that the sepiolite, in the polymerisation medium, has a noticeable effect not only on their thermal properties and stereoregularity, but also on the increase and narrowing of molecular weights of the nanocomposites, regardless of their tacticity.

These phenomena may be due to the stability that the sepiolite confers on the catalyst system, by protecting the active centres, that are on the surface of the support. Moreover, it is related to the strong influence of the supports on the propagation reactions, as already reported by some authors in other matrices, polymerized on supported metallocene catalysts [17,53,54].

In this sense, in a particular way it can be observed in the nanocomposites obtained with only one catalyst, that the sample N1sPP with a 3.2 wt% of effective clay has doubled its average molecular weight in number and weight (see Fig. 6a) in comparison with its counterpart without load (sPP). Although it follows the same trend, this result was not so spectacular in the synthesis of the iPP nanocomposite (See Fig. 6b). This shows that the nanoclay not only favours the formation of syndiotactic sections more, as demonstrated in section 3.1, but also, more markedly, favours an increase in the molecular weight of these sections. Despite the fact that these sections are formed with the C_s-symmetry catalyst, which is the most sensitive to impurities in the

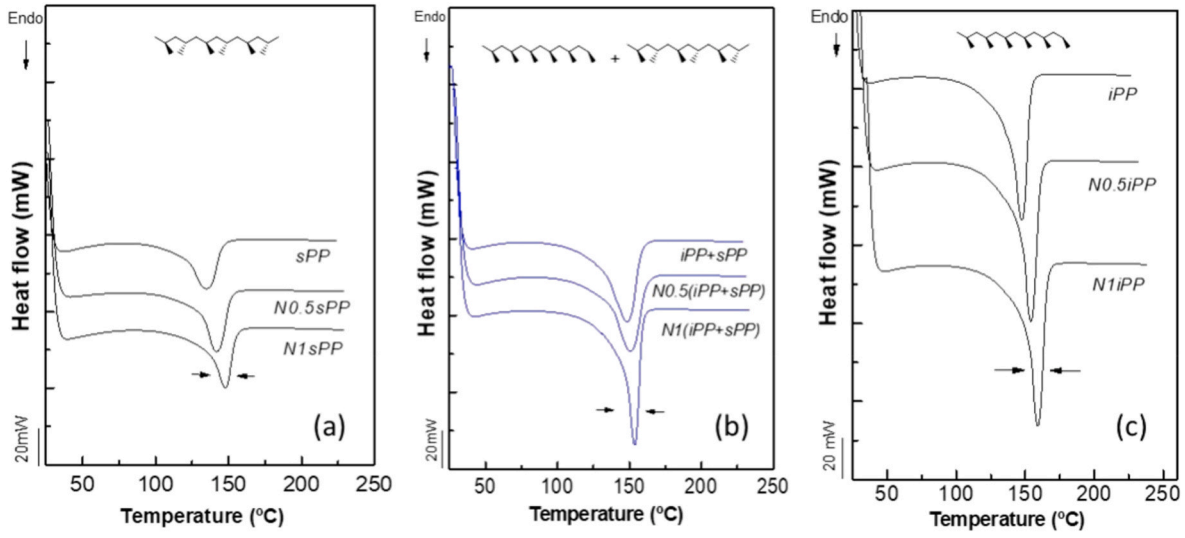

Fig. 4. Narrowing of the melting endotherms with increasing amount of nanoclay in (a) sPP (b) iPP + sPP and (c) iPP nanocomposites.

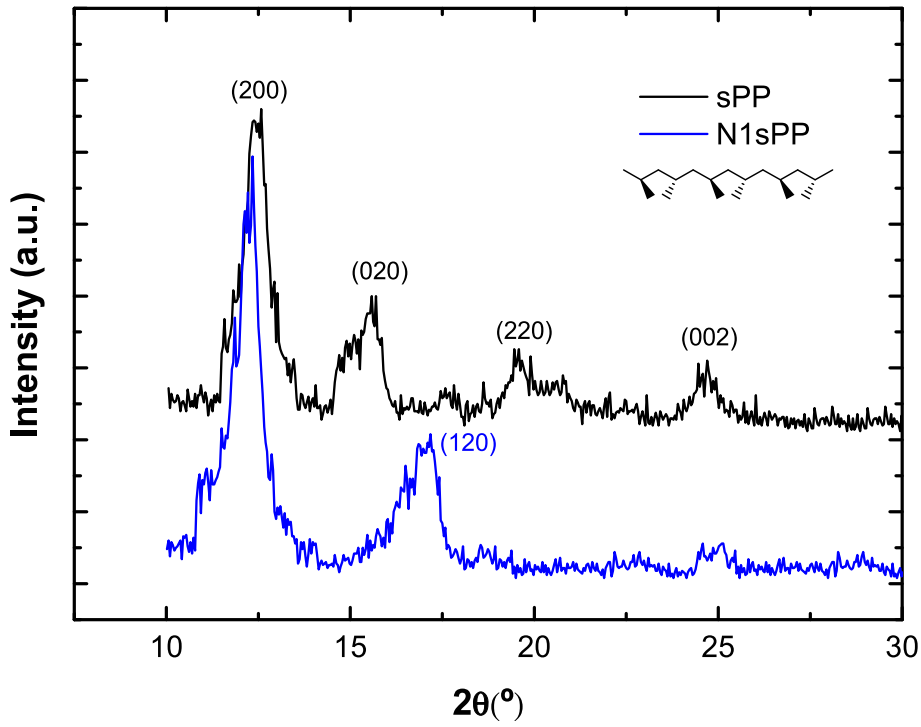

Fig. 5. WAXS pattern of sPP and its nanocomposite N1sPP.

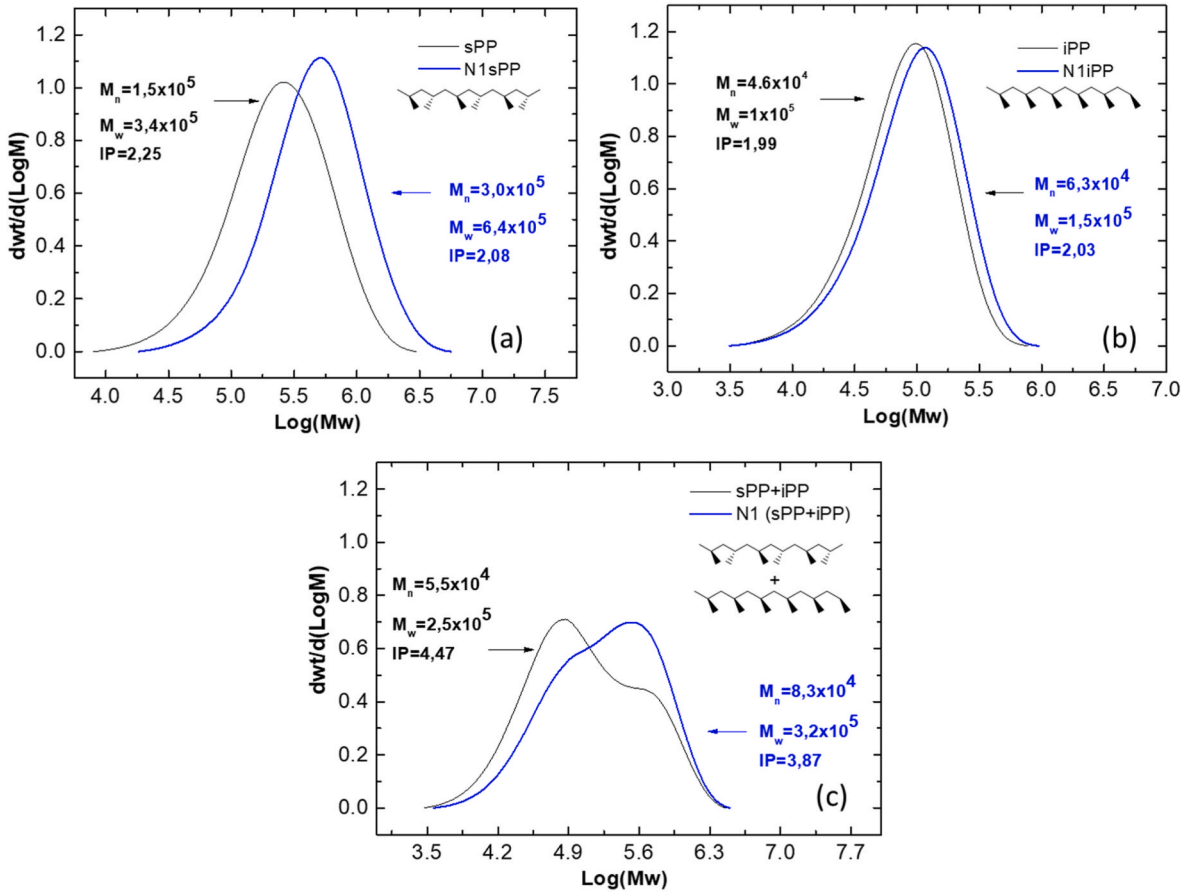

Fig. 6. Molecular weights (g/mol), distribution and podispersity by GPC test of (a) sPP, (b) iPP and (c) (iPP + sPP) and their nanoclay obtained with 1 g of initial nanoclay.

medium.

These increases and narrowing of molecular weights are also responsible for the thermal behaviour discussed above. Larger and narrower molecular weights and more stereospecific chains form a more regular crystalline population, also explained by the narrowing of the fusion endotherms shown in Fig. 4.

Additionally, our previous works [16,17,22] have shown that there is a threshold for the initial amount of nanofiller present in the metallocenic polyolefins polymerisation medium, above which productivity falls very abruptly and as the propagation reactions are not favoured due to the premature inactivity of the catalyst, polymer chains with sufficient molecular weight are not synthesized. Thereby the nucleating effect of the final nanofiller on these chains is not very effective. Below this threshold, very small amounts of sepiolite (<10 wt%) have an opposite effect: there is a significant increase in the molecular weight and the nucleating effect of the filler can be significant.

In the case of the catalysts studied here: sPP and mixtures (iPP + sPP), the threshold for the initial amount of nanofiller, in the studied condition, is close to 1 g, i.e, 4 wt% of final nanoclay. Polymerisation with larger final amounts of nanofiller was not possible, under the conditions studied, due to the extreme sensitivity of the Cs-symmetry catalyst activity, as has been demonstrated. This shows that the maximum potential of these materials obtained with the in-situ polymerisation technique, is found using very small amounts of nanoparticles, which means a great advantage in economic terms and weight reduction.

3.4. Mechanical properties

Young's specific modulus values and elongation at break are plotted as a function of polymerisation conditions (used catalyst and amount of nanofiller), see Fig. 7a. As expected in iPP nanocomposites, there is a large gap between the increase in stiffness and the loss of ductility as the clay amount is increased, obtaining very rigid materials but with low deformation capacity. Analysing sPP nanocomposites (see Fig. 7b), as a way to solve this disadvantage, it has been found not only an important improvement in Young's Modulus >50%, with 3.2% clay, but also that increase in stiffness goes, surprisingly, accompanied by an increase in the elongation at break >35% and maximum stresses. This is motivated by the significant increase in molecular weight and syndiotactic sections, in addition to an important increase in crystallinity and stiffness provided by having the highest percentage of clay in the final compound, as has already been demonstrated.

In the case of the catalyst mixture, a surprising effect was also obtained, although in negative terms. As the amount of nano-filler was increased, the Young's modulus decreased. The mixture of these catalysts has not shown a synergistic effect between the properties of these two types of PP tacticity that were studied, not even in its

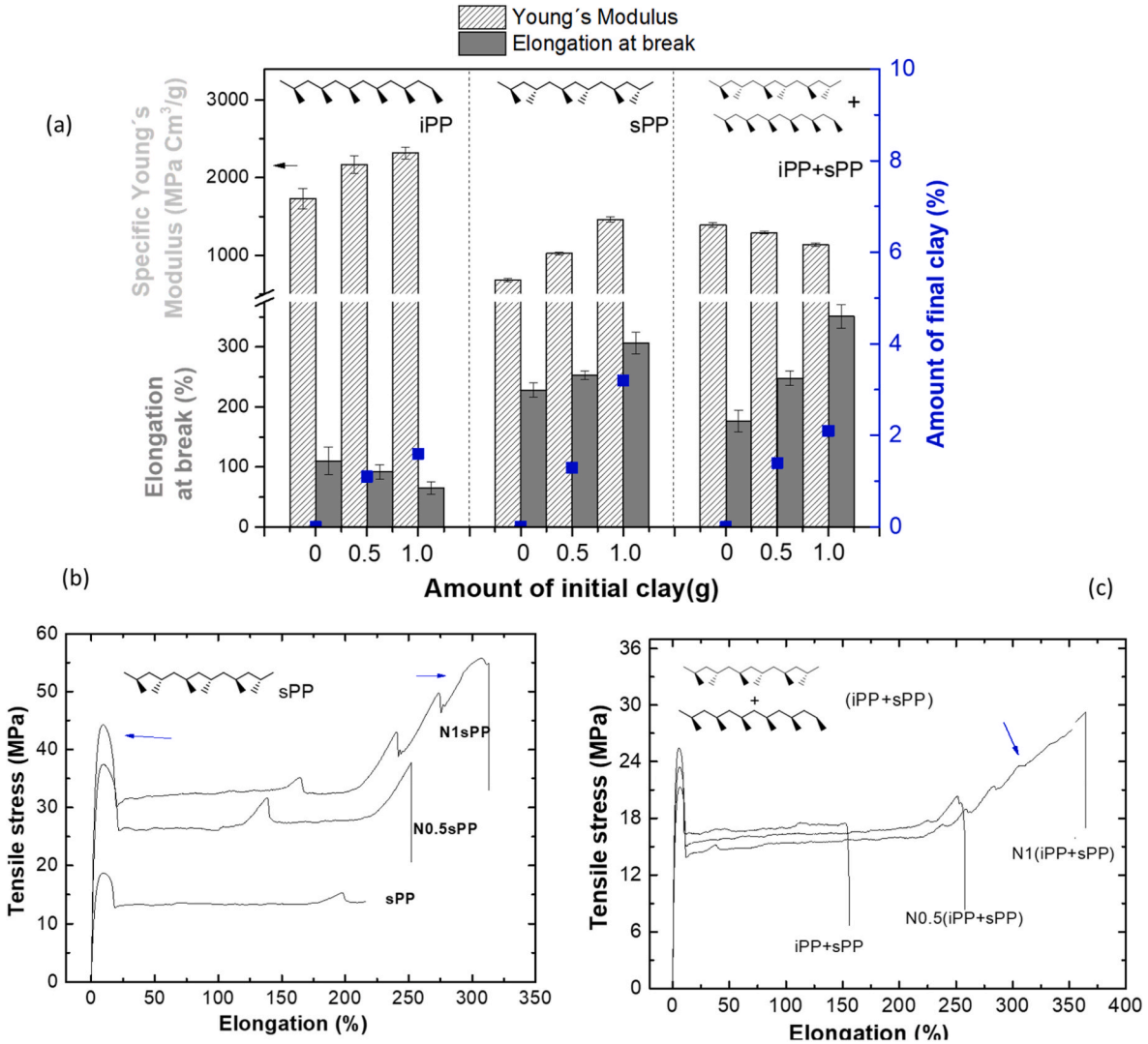

Fig. 7. (a) Mechanical properties of iPP, sPP, iPP + sPP and their nanocomposites, stress-strain curves of nanocomposites (b) sPP and (c) iPP + sPP.

nanocomposites. As shown in the thermal tests, this is clearly due to the clay did not manage to increase the crystallinity of the isotactical sections and, on the contrary, it was considerably reducing these sections to increase the syndiotacticity of the final compound, which finally achieved an increase in ductility of the material and a loss of rigidity. This is an evidence that the use of a nanoclay in the in-situ polymerisation does not always have a reinforcing effect because it also conditions the matrix that is formed.

An important aspect to highlight is that the nanocomposites synthesized in the presence of the C_s-symmetry catalyst (NsPP and N(iPP + sPP)) have shown a significant increase in resistance with deformation (see Fig. 7b and c).

During the tensile tests, a whitening of the deformed zone was observed, but there were no significant temperature changes when measuring the surface of the deformed specimen during the test. It was guessed that this change in the reflection of the material could indicate a molecular rearrangement associated with the phenomenon of strain-induced crystallization. Therefore, a first heating by DSC was performed to measure the differences between the deformed areas (whitish areas) and the non-deformed areas, no significant changes in the crystallinity of the samples were observed. It was then demonstrated that there is only strain hardening. The generation of a higher free volume in the syndiotactic configuration and in blends could be responsible for this higher molecular mobility. In Table 1 of the supporting information, it is possible to observe the values of the maximum tensile strength and the stress and strain at yield, for all the studied configurations.

Additionally, in the stress-strain curves of the sPP specimens, the mixture and its nanocomposites, the formation of certain "waves" can be observed as the tensile test progresses. These waves do not correspond to partial fracture or a partial release from machine grips, but to the formation of several necks in these specimens. Intense deformation occurs at both ends of the formed necks. As the test progresses, all the necks formed are joined together and the material as a whole tends to harden.

These behaviours seem to be due to the complex microstructure formed in the sPP nanocomposites and the mixture. Different crystalline structures undergo rearrangement, requiring different tensile stresses for their deformation. The shape of the curves demonstrates an effective stress transmission in the different crystalline structures formed through the amorphous sections that evolves according to the energy required by each crystalline system.

The formation of multiple necks in the studied nanocomposites may be due to the fact that the tensile test can induce crystalline regions to regroup and amorphous regions to crystallize as suggested by authors such as Wan et al. [55], for semicrystalline polymers. Additionally, also inhomogeneities within the bulk of the studied material may be responsible for the formation of these different necks. In addition, as the tensile test progresses, three modes of fracture in the periodic strips may be occurring: the micro-voids being formed in between microfibrils; the pull-out of the fibrils and crazing, which finally resulted in cavitation. The phenomenon of rearrangements and these partial cavitation mechanisms may explain the periodic changes in appearance in the form of transparent/opaque (whitening) bands in the deformed sample.

Finally, it is important to add that when the clay dispersion in the synthesized matrices was studied through TEM tests (see Fig. 8), the results showed that in the nanocomposites obtained with a mixture of catalysts there are a greater amount of clay aggregates (see Fig. 8c). These aggregates decrease the specific surface area of the nanoparticle, limiting its reinforcing ability. This could contribute to the low nucleating capacity of the nanofiller and the low stiffness of these nanocomposites.

4. Conclusion

To improve the mechanical properties of the NPPs, nanocomposites of different stereoregularity and their blends were synthesized by in-situ polymerisation.

The results showed that the iPP nanocomposites significantly increases the Young's modulus, due to their stereoregularity and to the nucleating effect of the clay in the medium, however, significant losses in elongation at break were reported. In the case of the sPP nanocomposites, despite the high sensitivity of the Cs-symmetry catalyst to medium impurities, remarkable changes in the microstructure were found with only 3 wt% of the final nanoclay. WAXS patterns, DSC and GPC assays showed an increase and narrowing of both molecular weights and melting endotherms, clearly showing a preference for unit cell type I hierarchical crystalline structures. Furthermore, an increase of 14% in stereoregularity were observed. This resulted in dramatic increases in Young's modulus and elongation at break with a sensitivity to molecular rearrangements during tensile testing.

Polymerisation with the mixture of catalyst resulted in blends that did not show significant synergies in the mechanical properties of the two configurations but demonstrated the preference of the polymerisation method used for the synthesis of syndiotactic sections.

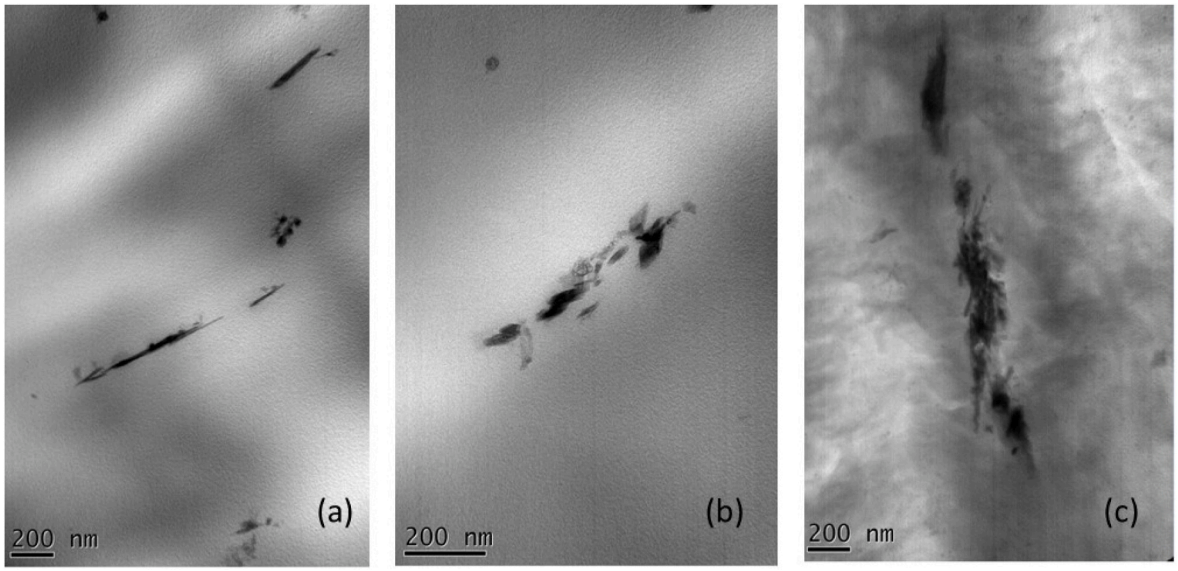

Fig. 8. Nanosepiolite aggregates observed in TEM micrographs on (a) N1iPP (b) N1sPP (c) N1(iPP + sPP).

CRediT authorship contribution statement

Karina Núñez: Methodology, Validation, Investigation, Data curation, Formal analysis, Writing – original draft. **Paolo Tanasi:** Investigation, Data curation, Formal analysis, Writing – original draft. **Maria Asensio:** Methodology, Validation, Resources, Data curation. **Manuel Herrero:** Conceptualization, Investigation, Writing – review & editing, Visualization, Supervision, Project administration. **Julia Guerrero:** Methodology, Visualization, Supervision. **José María Pastor:** Writing – review & editing, Supervision, Project administration, Funding acquisition.

Declaration of competing interest

The authors declare that they have no known competing financial interests or personal relationships that could have appeared to influence the work reported in this paper.

Acknowledgements

The authors acknowledge the financial support of "Ministerio de Economía y Competitividad – Spain" through the project PTQ-2018-009845 (M.H.) and PTQ2020-010968 (M A).

Appendix A. Supplementary data

Supplementary data to this article can be found online at https://doi.org/10.1016/j.polymer.2021.124480.

References

[1] N. Hasegawa, M. Kawasumi, M. Kato, A. Usuki, A. Okada, Preparation and mechanical properties of polypropylene - clay hybrids using a maleic, Macromolecules 30 (1997) 6333–6338.
[2] T. K, O.K. Arimitsu Usuki, Yoshitsugu Kojima, Masaya Kawasumi, Akane Okada, Yoshiaki Fukushima, Synthesis of nylon 6-clay hybrid, J. Mater. Res. 8 (1993) 1179–1184.
[3] M.M. Shameem, S.M. Sasikanth, R. Annamalai, R.G. Raman, A brief review on polymer nanocomposites and its applications, Mater. Today Proc. 45 (2021) 2536–2539, https://doi.org/10.1016/j.matpr.2020.11.254.
[4] C. Tsioptsias, K. Leontiadis, E. Tzimpilis, I. Tsivintzelis, Polypropylene nanocomposite fibers: a review of current trends and new developments, J. Plastic Film Sheeting (2020) 1–29, https://doi.org/10.1177/8756087920972146, 0.
[5] D.H. Kim, P.D. Fasulo, W.R. Rodgers, D.R. Paul, Effect of the ratio of maleated polypropylene to organoclay on the structure and properties of TPO-based nanocomposites. Part II: thermal expansion behavior, Polymer 49 (2008) 2492–2506, https://doi.org/10.1016/j.polymer.2008.04.005.
[6] Y. Xu, Z. Guo, Z. Fang, M. Peng, L. Shen, Combination of double-modified clay and polypropylene-graft-maleic anhydride for the simultaneously improved thermal and mechanical properties of polypropylene, J. Appl. Polym. Sci. 128 (2013) 283–291, https://doi.org/10.1002/app.38178.
[7] W. Lertwimolnun, B. Vergnes, Influence of compatibilizer and processing conditions on the dispersion of nanoclay in a polypropylene matrix, Polymer 46 (2005) 3462–3471, https://doi.org/10.1016/j.polymer.2005.02.018.
[8] R. Gallego, D. García-López, J.C. Merino, J.M. Pastor, How do the shape of clay and type of modifier affect properties of polymer blends? J. Appl. Polym. Sci. 127 (2013) 3009–3016, https://doi.org/10.1002/app.37979.
[9] G.Z. Papageorgiou, D.S. Achilias, D.N. Bikiaris, G.P. Karayannidis, Crystallization kinetics and nucleation activity of filler in polypropylene/surface-treated SiO2 nanocomposites, Thermochim. Acta 427 (2005) 117–128, https://doi.org/10.1016/j.tca.2004.09.001.
[10] W. Ren, K. Jayaraman, Blown films with balanced in-plane properties from polypropylene-clay nanocomposites though silane coupling, J. Plastic Film Sheeting 37 (2021) 93–110, https://doi.org/10.1177/8756087920939602.
[11] K. Hyun, H.T. Lim, K.H. Ahn, Nonlinear response of polypropylene (PP)/Clay nanocomposites under dynamic oscillatory shear flow, Korea Aust. Rheol. J. 24 (2012) 113–120, https://doi.org/10.1007/s13367-012-0013-2.
[12] H.G. Ock, K.H. Ahn, S.J. Lee, Effect of electric field on polymer/clay nanocomposites depending on the affinities between the polymer and clay, J. Appl. Polym. Sci. 133 (2016) 6–11, https://doi.org/10.1002/app.43582.
[13] M. Kim, H.Y. Song, W.J. Choi, K. Hyun, Evaluation of the degree of dispersion of polymer nanocomposites (PNCs) using nonlinear rheological properties by FT-rheology, Macromolecules 52 (2019) 8604–8616, https://doi.org/10.1021/acs.macromol.9b01302.
[14] F.C. Chiu, P.H. Chu, Characterization of solution-mixed polypropylene/clay nanocomposites without compatibilizers, J. Polym. Res. 13 (2006) 73–78, https://doi.org/10.1007/s10965-005-9009-7.
[15] X. Shi, Z. Gan, Preparation and characterization of poly(propylene carbonate)/montmorillonite nanocomposites by solution intercalation, Eur. Polym. J. 43 (2007) 4852–4858, https://doi.org/10.1016/j.eurpolymj.2007.09.024.
[16] P. Tanasi, M. Asensio, M. Herrero, K. Núñez, E. Cañibano, J.C. Merino, Control of branches distribution in linear PE copolymers using fibrillar nanoclay as support of catalyst system, Polymer (2020) 202, https://doi.org/10.1016/j.polymer.2020.122707.
[17] M. Herrero, K. Núñez, R. Gallego, J.C. Merino, J.M. Pastor, Control of molecular weight and polydispersity in polyethylene/needle-like shaped clay nanocomposites obtained by in situ polymerization with metallocene catalysts, Eur. Polym. J. 75 (2016) 125–141, https://doi.org/10.1016/j.eurpolymj.2015.12.005.
[18] W. Kaminsky, Polyole fi n-nanocomposites with special properties by in-situ polymerization, Chem. Sci. Eng. 12 (2018) 555–563.
[19] B.M. Cromer, S. Scheel, G.A. Luinstra, E.B. Coughlin, A.J. Lesser, In-situ polymerization of isotactic polypropylene-nanographite nanocomposites, Polymer 80 (2015) 275–281, https://doi.org/10.1016/j.polymer.2015.09.074.
[20] O.M. Palaznik, P.M. Nedorezova, V.G. Shevchenko, V.G. Krasheninnikov, T. V. Monakhova, A.A. Arbuzov, Synthesis and properties of polymerization-filled composites based on polypropylene and single-wall carbon nanotubes, Polym. Sci. B 63 (2021) 138–151, https://doi.org/10.1134/S1560090421020093.
[21] R.S. Cardoso, V.O. Aguiar, M. de F.V. Marques, Masterbatches of polypropylene/clay obtained by in situ polymerization and melt-blended with commercial polypropylene, J. Compos. Mater. 51 (2017) 3547–3556, https://doi.org/10.1177/0021998317690444.
[22] M. Asensio, M. Herrero, K. Núñez, R. Gallego, J.C. Merino, J.M. Pastor, In situ polymerization of isotactic polypropylene sepiolite nanocomposites and its copolymers by metallocene catalysis, Eur. Polym. J. 100 (2018) 278–289, https://doi.org/10.1016/j.eurpolymj.2018.01.034.
[23] C. De Rosa, F. Auriemma, Structure and physical properties of syndiotactic polypropylene: a highly crystalline thermoplastic elastomer, Prog. Polym. Sci. 31 (2006) 145–237, https://doi.org/10.1016/j.progpolymsci.2005.11.002.
[24] F. Endo, R. Okoshi, K. Takaesu, N. Kurokawa, H. Iwase, T. Maeda, A. Hotta, Mechanically tough syndiotactic polypropylene (sPP) gels realized by fast quenching using liquid nitrogen, Macromolecules 51 (2018) 2321–2327, https://doi.org/10.1021/acs.macromol.7b02426.
[25] X. Wang, J. Yi, L. Wang, Y. Yuan, J. Feng, Thermorheological evidence and structure of heterogeneity in syndiotactic polypropylene melts with strong memory effects, Polymer 218 (2021) 123484, https://doi.org/10.1016/j.polymer.2021.123484.
[26] F. Auriemma, C. De Rosa, New concepts in thermoplastic elastomers: the case of syndiotactic polypropylene, an unconventional elastomer with high crystallinity and large modulus, J. Am. Chem. Soc. 125 (2003) 13143–13147, https://doi.org/10.1021/ja036282v.
[27] R. Cipullo, A. Vittoria, V. Busico, Assignment of regioirregular sequences in the 13C NMR spectrum of syndiotactic polypropylene, Polymers 10 (2018), https://doi.org/10.3390/polym10080863.
[28] F. Auriemma, C. De Rosa, A. Malafronte, M. Scoti, Di Girolamo, Solid state polymorphism of isotactic and syndiotactic polypropylene, in: Polypropylene Handbook, Morphology, Blends and Composites, 2019, https://doi.org/10.5860/choice.43-2825.
[29] M. Scoti, R. Di Girolamo, G. Giusto, F. De Stefano, F. Auriemma, A. Malafronte, G. Talarico, C. De Rosa, Mechanical properties and elastic behavior of copolymers of syndiotactic polypropylene with 1 - Hexene and 1 - Octene. https://doi.org/10.1021/acs.macromol.1c00892, 2021.
[30] L.T. Truong, Å.G. Larsen, J. Roots, Morphology, crystalline features, and tensile properties of syndiotactic polypropylene blends, J. Appl. Polym. Sci. 134 (2017) 1–10, https://doi.org/10.1002/app.44611.
[31] L.T. Truong, Á. Larsen, B. Holme, F.K. Hansen, J. Roots, Morphology of syndiotactic polypropylene/alumina nanocomposites, Polymer 52 (2011) 1116–1123, https://doi.org/10.1016/j.polymer.2011.01.014.
[32] J. Bejarano, R. Benavente, E. Pérez, M. Wilhelm, R. Quijada, H. Palza, Effect of polymer structure and incorporation of nanoparticles on the behavior of syndiotactic polypropylenes, Macromol. Chem. Phys. 214 (2013) 2567–2578, https://doi.org/10.1002/macp.201300392.
[33] A.Z.H. Palza, Effect of the polymer microstructure on the behavior of syndiotactic polypropylene/organophilic layered silicate composites, J. Appl. Polym. Sci. 124 (2011) 2601–2609, https://doi.org/10.1002/app.
[34] G. Gorrasi, M. Tortora, V. Vittoria, D. Kaempfer, R. Mülhaupt, Transport properties of organic vapors in nanocomposites of organophilic layered silicate and syndiotactic polypropylene, Polymer 44 (2003) 3679–3685, https://doi.org/10.1016/S0032-3861(03)00284-2.
[35] Z. Mlynarčíkoá, D. Kaempfer, R. Thomann, R. Mülhaupt, E. Borsig, A. Marcinčin, Syndiotactic poly(propylene)/organoclay nanocomposite fibers: influence of the nano-filler and the compatibilizer on the fiber properties, Polym. Adv. Technol. 16 (2005) 362–369, https://doi.org/10.1002/pat.602.
[36] D. Kaempfer, R. Thomann, R. Mülhaupt, Melt compounding of syndiotactic polypropylene nanocomposites containing organophilic layered silicates and in situ formed core/shell nanoparticles, Polymer 43 (2002) 2909–2916, https://doi.org/10.1016/S0032-3861(02)00113-1.
[37] N. Ahmad, E. Fouad, Influence of clay contents on rheology of syndiotactic polypropylene/clay composites, Arabian J. Sci. Eng. 42 (2017) 1537–1543, https://doi.org/10.1007/s13369-016-2389-7.
[38] V.G. Gregoriou, G. Kandilioti, S.T. Bollas, Chain conformational transformations in syndiotactic polypropylene/layered silicate nanocomposites during mechanical elongation and thermal treatment, Polymer 46 (2005) 11340–11350, https://doi.org/10.1016/j.polymer.2005.10.026.

[39] S.V. Polshchikov, P.M. Nedorezova, O.M. Komkova, A.N. Klyamkina, A. N. Shchegolikhin, V.G. Krasheninnikov, A.M. Aladyshev, V.G. Shevchenko, V. E. Muradyan, Synthesis by polymerization in situ and properties of composite materials based on syndiotactic polypropylene and carbon nanofillers, Nanotechnologies Russ 9 (2014) 175–183, https://doi.org/10.1134/S1995078014020128.

[40] K. Núñez, R. Gallego, J.M. Pastor, J.C. Merino, Applied Clay Science the structure of sepiolite as support of metallocene co-catalyst during in situ polymerization of polyole fi n (nano) composites, Appl. Clay Sci. 101 (2014) 73–81, https://doi.org/10.1016/j.clay.2014.07.020.

[41] C.A.K. Núñez, R. Gallego, J.C. Merino, J.M. Pastor, WO2013-167764A1 Procedimiento de polimerización sobre nanopartículas y polímero así obtenido, Fundación Cidaut, Spain, 2012.

[42] S. Bourbigot, L. Garnier, B. Revel, S. Duquesne, Characterization of the morphology of iPP/sPP blends with various compositions, Express Polym. Lett. 7 (2012) 224–237, https://doi.org/10.3144/expresspolymlett.2013.21.

[43] M.C. de O. Maria de Fatima Vieira Marques, Polypropylene nanocomposites using metallocene catalysts supported on commercial organophilic clays, Polym. Bull. 64 (2010) 221–231, https://doi.org/10.1007/s00289-009-0138-8.

[44] W. Wang, Z. Fan, Y. Zhu, Y. Zhang, L. Feng, Effects of cocatalyst on structure distribution of propylene polymers catalyzed by rac -Me 2 Si, Ind) 2 ZrCl 2/ aluminoxane 38 (2002) 1551–1558.

[45] R. Thomann, Y. Thomann, R. Mülhaupt, J. Kressler, K. Busse, D. Lilge, J.C. W. Chien, Morphology of stereoblock polypropylene, J. Macromol. Sci. Phys. 41 B (2002) 1079–1090, https://doi.org/10.1081/MB-120013085.

[46] A.A. Kovalchuk, V.G. Shevchenko, A.N. Shchegolikhin, P.M. Nedorezova, A. N. Klyamkina, A.M. Aladyshev, Isotactic and syndiotactic polypropylene/multi-wall carbon nanotube composites: synthesis and properties, J. Mater. Sci. 43 (2008) 7132–7140, https://doi.org/10.1007/s10853-008-3029-8.

[47] E. López-Moya, R. van Grieken, A. Carrero, B. Paredes, Influence of stereospecificity and molecular weight on mechanical properties of iso-syndio-polypropylene obtained by combination of metallocene catalysts, Eur. Polym. J. 90 (2017) 183–194, https://doi.org/10.1016/j.eurpolymj.2017.03.019.

[48] V. Vittoria, L. Guadagno, A. Comotti, R. Simonutti, F. Auriemma, C. De Rosa, Mesomorphic form of syndiotactic polypropylene, Macromolecules 33 (2000) 6200–6204, https://doi.org/10.1021/ma000373k.

[49] M. de F.V. Marques, C.C. Pombo, R.A. Silva, A. Conte, Binary metallocene supported catalyst for propylene polymerization, Eur. Polym. J. 39 (2003) 561–567, https://doi.org/10.1016/S0014-3057(02)00269-0.

[50] Q.C. Bastos, M. De Fátima Vieira Marques, Polypropylene reactor mixture obtained with homogeneous and supported catalysts, J. Polym. Sci. Part A Polym. Chem. 43 (2005) 263–272, https://doi.org/10.1002/pola.20494.

[51] A. Tynys, T. Saarinen, M. Bartke, B. Löfgren, Propylene polymerisations with novel heterogeneous combination metallocene catalyst systems, Polymer 48 (2007) 1893–1902, https://doi.org/10.1016/j.polymer.2007.02.020.

[52] F. Stricker, R.D. Maier, M. Bruch, R. Thomann, R. Mülhaupt, Influence of glass bead fillers on phase transitions of syndiotactic polypropene, Polymer 40 (1999) 2077–2084, https://doi.org/10.1016/S0032-3861(98)00247-X.

[53] W. Li, A. Adams, J. Wang, B. Blümich, Y. Yang, Polyethylene/palygorskite nanocomposites : preparation by in situ polymerization and their characterization, Polymer 51 (2010) 4686–4697, https://doi.org/10.1016/j.polymer.2010.08.037.

[54] C. Covarrubias, E. Moncada, J. Retuert, P. Zapata, Catalytic activity during the preparation of PE/clay nanocomposites by in situ polymerization with metallocene catalysts, J. Appl. Polym. Sci. 113 (2009) 2368–2377, https://doi.org/10.1002/app.

[55] C. Wan, E.L. Heeley, Y. Zhou, S. Wang, C.T. Cafolla, E.M. Crabb, D.J. Hughes, Stress-oscillation behaviour of semi-crystalline polymers: the case of poly(butylene succinate), Soft Matter 14 (2018) 9175–9184, https://doi.org/10.1039/C8SM01889H.